Acta Pharmaceutica Sinica B 2018;8(1):116–126

Chinese Pharmaceutical Association
Institute of Materia Medica, Chinese Academy of Medical Sciences

Acta Pharmaceutica Sinica B

www.elsevier.com/locate/apsb
www.sciencedirect.com

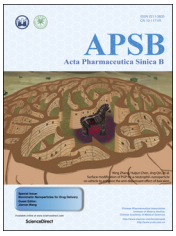

ORIGINAL ARTICLE

Improved method for synthesis of low molecular weight protamine–siRNA conjugate

Zhili Yu[a,†], Junxiao Ye[b,†], Xing Pei[a], Lu Sun[a], Ergang Liu[c], Jianxin Wang[d,e], Yongzhuo Huang[f], Seung Jin Lee[g], Huining He[a,*]

[a]*Tianjin Key Laboratory on Technologies Enabling Development of Clinical Therapeutics and Diagnostics, School of Pharmacy, Tianjin Medical University, Tianjin 300070, China*
[b]*College of Pharmacy, Tsinghua University, Beijing 100084, China*
[c]*Collaborative Innovation Center of Chemical Science and Chemical Engineering and Technology, Tianjin University, Tianjin 300072, China*
[d]*Key Laboratory of Smart Drug Delivery, Ministry of Education & PLA, Shanghai 201201, China*
[e]*Department of Pharmaceutics, School of Pharmacy, Fudan University, Ministry of Education & PLA, Shanghai 201201, China*
[f]*Shanghai Institute of Materia Medica, Chinese Academy of Sciences, Shanghai 201203, China*
[g]*Department of Pharmacy, Ewha Womans University, Seodaemun-gu, Seoul 120-750, Republic of Korea*

Received 26 August 2017; received in revised form 21 September 2017; accepted 10 November 2017

KEY WORDS

Cell penetrating peptide;
siRNA;
Conjugate;
Conjugation yield;
Biomimetic delivery;
Crosslinker

Abstract RNAi technology has aroused wide public interest due to its high efficiency and specificity to treat multiple types of diseases. However, the effective delivery of siRNA remains a challenge due to its large molecular weight and strong anionic charge. Considering their remarkable functions *in vivo* and features that are often desired in drug delivery carriers, biomimetic systems for siRNA delivery become an effective and promising strategy. Based on this, covalent attachment of synthetic cell penetrating peptides (CPP) to siRNA has become of great interest. We developed a monomeric covalent conjugate of low molecular weight protamine (LMWP, a well-established CPP) and siRNA *via* a cytosol-cleavable disulfide linkage using PEG as a crosslinker. Results showed that the conjugates didn't generate coagulation, and exhibited much better RNAi potency and intracellular delivery compared with the conventional charge-complexed CPP/siRNA aggregates. Three different synthetic and purification methods were compared in order to optimize synthesis efficiency and product yield. The methodology using hetero-bifunctional NHS–PEG–OPSS as a crosslinker to

*Corresponding author. Tel./fax: +86 22 83336658.
E-mail address: hehuining@tmu.edu.cn (Huining He).
†These authors made equal contributions to this work.
Peer review under responsibility of Institute of Materia Medica, Chinese Academy of Medical Sciences and Chinese Pharmaceutical Association.

https://doi.org/10.1016/j.apsb.2017.11.011

synthesize LMWP–siRNA simplified the synthesis and purification process and produced the highest yield. These results pave the way towards siRNA biomimetic delivery and future clinical translation.

1. Introduction

Post-transcriptional gene silencing occurs naturally in a process called RNA interference (RNAi), first reported by Fire and Mello in 1998[1]. RNAi holds promise as a powerful tool for gene therapy for novel treatments of various diseases[2–5]. RNAi is triggered by double-stranded RNA (dsRNA), after which dsRNA is cleaved by dicer, a member of the RNase III family of ribonucleases, to generate 21–23 double-stranded short interfering RNA duplexes (siRNA)[6]. Due to the high efficiency, specificity and the ability to perform numerous rounds of mRNA cleavage, siRNA has been recognized as the most attractive candidates for modulating disease-related mRNAs[7–9]. The site of action of siRNA is the cytosol. However, since polyanionic siRNAs are large molecules (MW: 1.3×10^4 to 1.5×10^4 Da) with negative charges from the phosphate backbone (about –40 charges)[10], they cannot readily enter cells by passive diffusion. In addition, nuclease susceptibility and poor penetration into many tissues are also biological barriers to siRNA delivery[11]. To realize its therapeutic potential, it is important to establish an efficient siRNA biomimetic delivery system.

Biomimetic drug delivery systems based on natural particulate range from pathogens to mammalian cells, as they possess specific functions *in vivo* that are worth examining in more depth. In conjunction with the availability of advanced biotechnology tools, investigators have exploited natural particulates for multiple applications in the delivery of proteins, siRNA and other therapeutic agents. For siRNA delivery, the biomimetic systems are generally divided into two major types based on viral and non-viral vectors. The viral systems use transfection of shorthairpin RNA (shRNA)-expressing vectors to produce siRNA in a cell[12]. However, one of the major problems of the viral vector system is the unwanted side effects that are caused by off-target reactions due to the natural tropism[13], even if it has a high efficiency for siRNA delivery. A wide range of non-viral vectors systems including liposome and lipids[14,15], cholesterol-conjugated[16], cationic polymers[17], RNA aptamers[18] and peptides[19] have been developed for siRNA delivery. These non-viral systems with improved safety, reduced immunogenicity, enhanced efficacy on target sites have shown potential for applications in biomimetic siRNA delivery. Among these, cell penetrating peptide (CPP) -mediated siRNA delivery is noteworthy. CPPs are capable of carrying a wide range of macromolecules into a variety of cells, with less cytotoxicity and high efficiency.

In general, biomimetic siRNA delivery mediated by CPP mainly occurs through two strategies, by noncovalently complexed *via* charge interactions[20] or by covalent conjugation[21]. Most of the studies involving CPPs have utilized the non-covalent conjugation method. The formation of noncovalent electrostatic complexes is a technically simple approach, and it may induce effective intracellular uptake. However, the formulation process of covalent conjugates can be well controlled in terms of homogeneity and reproducibility[22]. Besides, CPP-mediated transport efficiency of the covalent compound is higher than that of physical mixtures[23–25].

To achieve the efficient siRNA biomimetic delivery that vectorized with CPPs, it is necessary to formulate a soluble, 1:1 monomeric CPP–siRNA conjugate through a cytosol-cleavable disulfide linkage. After the siRNA is deliveried by the CPP into the cell, the siRNA can be retained in the cytosol with the disulfide linkage cleaved in the reductive enviroment, performing gene silencing treatment function through the RNA-induced silencing complex (RISC) system. PEGylation is known to have a shielding effect on charged molecules and reduce host immune response, so that PEG was introduced as a crosslinker. It has been shown that the conjugates did not generate coagulation, yet exhibited much better RNAi potency and intracellular delivery compared with the conventional charge-complexed CPP/siRNA aggregates[26].

In the present study, the abovementioned conjugation method was further improved in order to simplify the process and increase the yield. As depicted in Scheme 1, three methods were applied with either different purification steps or different linkers. We aimed to find a method combining efficient synthesis and purification steps with the highest production yields.

2. Materials and methods

2.1. Materials

LMWP (VSRRRRGGRRRRRR) was produced according to our developed protocol[27,28]. Heterobifunctional PEG derivatives maleimide PEG succinimidyl carboxymethyl ester (MW = 3500 Da) and ortho-pyridyl disulfide PEG succinimidyl carboxymethyl ester (MW = 3500 Da) were purchased from Jenkem technology Co., Ltd. (Beijing, China). Anti-enhanced green fluorescent protein (EGFP) siRNA–cysteine was synthesized by Guangzhou Ribobio Co., Ltd. (Guangzhou, China). The sense and anti-sense strands of siRNA was: 5′-GGCUACGUCCAGGAGCGCACC-3′ (sense), 3′-UUCCGAUGCAGGUCCUCGCGU-5′(anti-sense). For coupling, the sense strand of the siRNA was modified with an extra cysteine residue at its 5′-end. *N*-Succinimidyl 3-(2-pyridyldithio) propionate (SPDP) and dithiothreitol (DTT) were purchased from Thermo–Fisher Scientific Inc. Dimethyl sulfoxide (anhydrous solvent) was bought from Aladdin Industrial Corporation (Shanghai, China). Hi-Trap heparin™ HP columns, Hi-Trap™ DEAE FF columns, DEAE Sepharose Fast Flow were obtained from GE Healthcare Bio-Sciences Corp (Stockholm, Sweden). Affinity columns were obtained from Sangon Biotech (Shanghai, China). Agrose B, low EEO (Biotech Grade), was supplied by BBI Life Sciences Corporation (Shanghai, China). 20 bp DNA ladder, nucleic acid dyestuffs SYGR GreenII, 6 × DNA loading buffer and poly-lysine were purchased from Beijing Solarbio Science & Technology Co., Ltd. (Beijing, China). 5-(and-6)-Carboxytetramethylrhodamine, succinimdyl ester (TAMRA) was from AnaSpec Inc. (CA, USA). 4′,6-Diamidino-2-phenylindole (DAPI) and paraformaldehyde were from Sigma–Aldrich (St. Louis, MO,

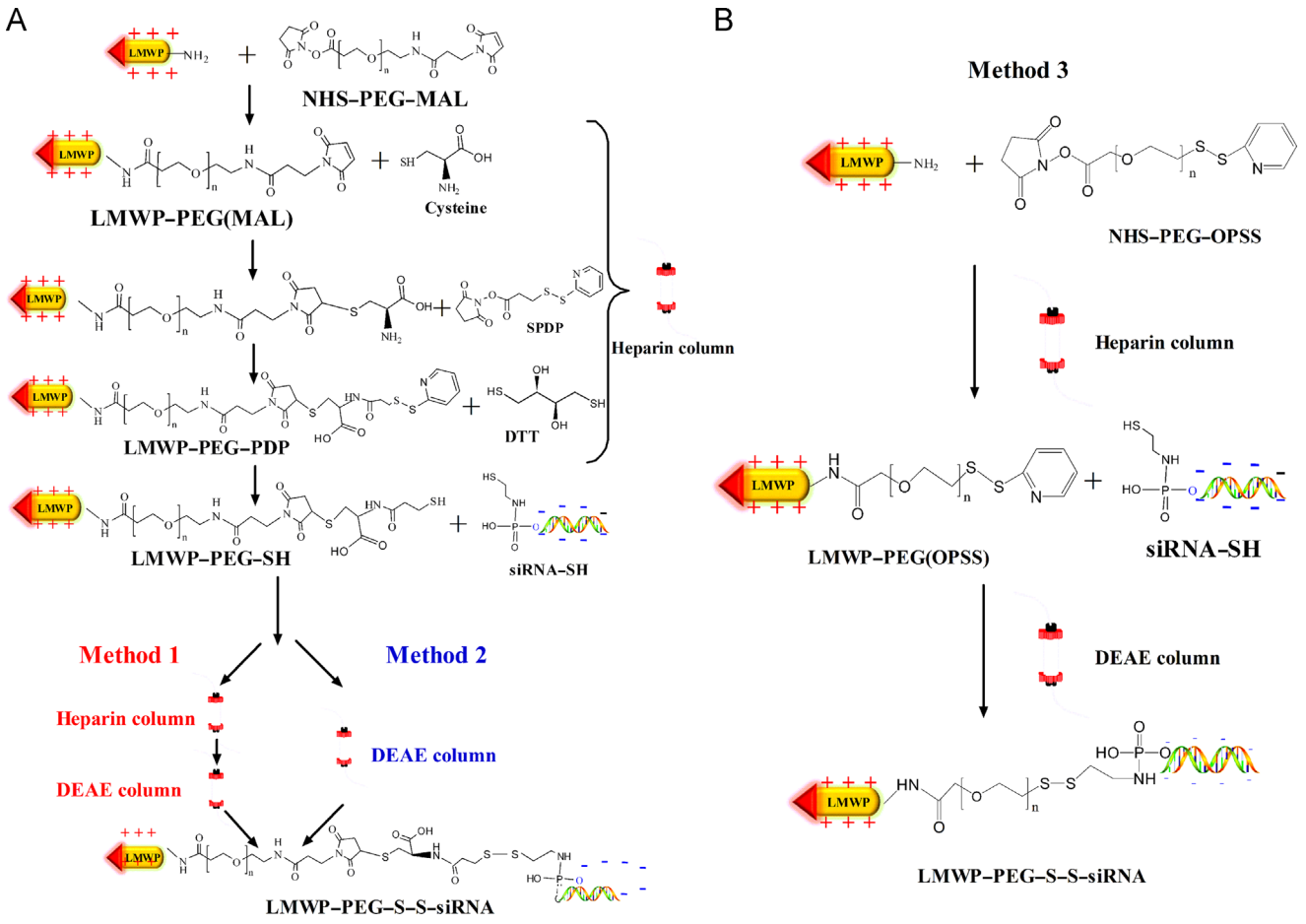

Scheme 1 Synthesis and purification scheme of the LMWP–PEG–siRNA conjugate. (A) NHS–PEG–MAL was introduced to synthesize the conjugate and the crude LMWP–PEG–S–S–siRNA product was purified by two methods: (1) Heparin column and DEAE column in two steps (Method 1); (2) DEAE column in one step (Method 2). (B) NHS–PEG–OPSS was introduced to synthesize the conjugate, while the LMWP–PEG (OPSS) compound was purified through heparin column and the final conjugate was purified by DEAE column (Method 3).

USA). Human colon cancer cell line HCT 116 was obtained from Chinese Academy of Sciences Typical Culture Collection (Shanghai, China). EGFP stably transfected cell line, MDA-MB-231-EGFP cells, were kindly donated by Prof. Xiaoyue Tan (School of Medicine, Nankai University, Tianjin, China). All of the cell culture reagents were purchased from Thermo–Fisher Scientific Inc. Diethypyrocarbonate (DEPC) was supplied by Beyotime Institute of Biotechnology (Beijing, China). Water was distilled and deionized. Unless otherwise stated, chemicals were purchased from Sinopharm chemical reagent Beijing Co. (Beijing, China).

2.2. *Synthesis of LMWP–PEG–S–S–siRNA conjugate*

LMWP–PEG(MAL)–siRNA conjugate was synthesized according to our previous study[26]. Briefly, LMWP was first linked with the hetero-bifunctional PEG derivatives NHS–PEG–MAL to yield LMWP–PEG(MAL) conjugate. Then coupled to cysteine thus formed the LMWP–PEG–NH_2 conjugate. It was then activated with SPDP and thiolated with DTT to yield a reactive LMWP–PEG–SH compound. After that, 5′-sulfhydryl siRNA was added to the afore-activated LMWP–PEG–SH to yield the LMWP–PEG (MAL)–siRNA final conjugate.

Alternatively, LMWP was amino-terminally coupled to a short (~3500 Da) hetero-bifunctional PEG chain containing activated ends of succinimidyl carboxymethyl ester (NHS ester) and ortho-pyridyl disulfide (OPSS) in phosphate buffer. The LMWP was modified at its N-terminus with the NHS-end of the PEG polymer. As ortho-pyridyl disulfide reacts with thiol group to form a stable disulfide bond, 5′-sulfhydryl siRNA was then added to the LMWP–PEG(OPSS) conjugate to yield the LMWP–PEG (OPSS)–siRNA conjugate.

The yields of the LMWP compounds in each step were obtained by integrating the absorption peak area that detected at a wavelength of 215 nm. The concentration of the siRNA was measured with Themo Scientific μDrop Plate and calculated on the basis of absorbance at 260 nm wavelength. The yields of LMWP compounds and siRNA were determined using the following Eq. (1):

$$\text{Yield}_{\text{LMWP compound}}\,(\%) = \frac{A_{\text{LMWP compound}}}{A_{\text{LMWP compound}} - A_{\text{Unreacted products}}} \times 100 \quad (1)$$

$$\text{Yield}_{\text{siRNA}}\,(\%) = \frac{C_{\text{siRNA}} \times V_{\text{Conjugate}}}{\text{Total input of siRNA}} \times 100 \quad (2)$$

where $A_{\text{LMWP compound}}$, $A_{\text{Unreacted products}}$ represent the peak area of LMWP compound and unreacted products, while C_{siRNA}, $V_{\text{Conjugate}}$

represent the concentration of siRNA, and the volume of conjugate, respectively.

2.3. Purification and characterization of LMWP–PEG–S–S–siRNA conjugate

The purification approaches are displayed in Scheme 1 for all three methods. For all the purification steps when producing the LMWP–PEG–SH compound in Method 1 and Method 2, cationic exchange Hi-Trap heparin TM HP (1 mL, GE Healthcare, Sweden) columns were applied using 20 mmol/L sodium phosphate solution containing 10 mmol/L EDTA at pH 7.2 (solution A) as the equilibrium buffer and the same solution containing 2 mol/L NaCl (solution B) as the elution buffer. The elution conditions for each step before obtaining the LMWP–PEG–SH compounds were as follows: flow rate: 1 mL/min; detection wavelength: 215 nm. A linear gradient from 0 to 100% solution B was used to purify LMWP–PEG(MAL) compound. In the subsequent purification process, isocratic elution was carried on.

The difference between Method 1 and Method 2 are seen in the purification of the LMWP–PEG–S–S–siRNA conjugate. For Method 1, the crude product was purified through two steps of heparin column and anion exchange chromatography Hi-Trap DEAE^{TM} FF (1 mL, GE Healthcare, Sweden). When the conjugate was purified on heparin column, the elution conditions were similar to those described above, only with the detection wavelength being set at 260 nm. The DEAE column was then used for purification with the following conditions: equilibrium buffer: 20 mmol/L sodium phosphate, pH = 8.9; elution buffer: 20 mmol/L sodium phosphate, 2 mol/L NaCl, pH = 8.9; flow rate: 1 mL/min; linear gradient: 0–60% of solution B; detection wavelength: 260 nm. For Method 2, on the other hand, only one step purification through DEAE column was applied[26].

For Method 3, purification of the LMWP–PEG(OPSS) conjugate was simplified to a single step using heparin column with detection wavelength at 215 nm using a gradient starting from 0% B to 100% B (buffer A, 20 mmol/L sodium phosphate buffer at pH 6.9; buffer B, 20 mmol/L sodium phosphate buffer containing 2 mol/L NaCl at pH 6.9) at a flow rate of 1 mL/min. Then the final conjugate was purified by DEAE column. Equilibrium buffer were 20 mmol/L sodium phosphate solution containing 1 mmol/L EDTA at pH 6.9 (buffer A) and the same ingredient containing 1 mol/L NaCl (buffer B) as elution buffer. The column was eluted at a flow rate of 1 mL/min, meanwhile the NaCl gradient was increased from 0 to 0.7 mol/L. The elution of the sample solution was detected at 260 nm.

To characterize the products, LMWP–PEG, physical mixture, naked siRNA and the conjugates containing equal amount of siRNA were mixed with 6 × gel loading buffer, applied on the 2% agarose gel and run at 80 V/cm for 30 min at room temperature followed by SYGR Green II staining and Coomassie Brilliant Blue staining, then visualization under UV light.

The matrix-assisted laser desorption/ionization time of fight (MALDI-TOF) mass spectrometry was also used for characterization of the purified conjugates, according to a well-established procedure[29].

2.4. Particle size and ζ-potential of LMWP–PEG–S–S–siRNA conjugates

The size of freshly prepared LMWP–PEG–S–S–siRNA conjugate was measured by dynamic light scattering. Samples solutions were pipetted into UV cuvette and sizes were determined at room temperature in a Nano ZS Zetasizer (Malvern Instruments, Malvern, UK). ζ-Potentials were measured in the same machine. To that end, freshly prepared samples were slowly injected into a folded capillary ζ-potential cuvette. Freshly prepared samples contained 10% FBS for measurements in serum conditions. Both size and ζ-potential mean values were determined from three independent measurements. As controls, physical mixture (N/P = 1:1), physical mixture (N/P = 10:1) were measured. (N = positively charged amino acids, P = phosphate groups on siRNA).

2.5. Serum stability of LMWP–PEG–S–S–siRNA conjugates

For siRNA stability estimation, LMWP–PEG–S–S–siRNA conjugate was diluted 1:10 with DMEM+10% FBS and then incubated at 37 °C for indicated timespans, followed by 2% agarose gel electrophoresis and SYGR Green II staining. As control, the conjugate was diluted 1:10 with phosphate buffer, and was observed under the UV light of the gel imager.

2.6. Cellular uptake of LMWP–PEG–S–S–siRNA conjugates

Human colon cancer HCT 116 cells were maintained in McCoy's 5a medium supplemented with 10% FBS and 1% penicillin–streptomycin at 37 °C in a humidified atmosphere of 5% CO_2. The coverslips were pretreated with poly-lysine and air drying overnight. Cells were plated on coverslips at a density of 5×10^4 cells/coverslip and incubated until complete adhesion. Then the culture medium was removed. Treatments were as follows: PBS, TAMRA-labeled native siRNA and TAMRA-labeled LMWP–PEG(OPSS)–siRNA. After incubated with the HCT 116 cells at 37 °C for 4 h, cells were washed with PBS carefully and fixed with 4% paraformaldehyde for 30 min, further incubated with the DAPI (5 μg/mL) to visualize nucleus. Cellular uptake was assayed by excitation of TAMRA at 565 nm and detection of emission at 580 nm. An Olympus FV-1000 laser scanning microscope was used to collect the images and data were analyzed and operated with FLUOVIEW software (Olympus, Tokyo, Japan).

2.7. Gene silencing efficacy of LMWP–PEG–S–S–siRNA conjugates

Flow cytometry (BD Biosciences, Bradford, MA, USA) was used to evaluate the effect of conjugate gene silencing. Briefly, the EGFP stable transfected cell line MDA-MB-231-EGFP cells were treated with PBS, naked siRNA, LMWP–PEG–S–S–siRNA conjugate, and incubated for 12 h, followed by the replacement with fresh culture media and further incubation for 72 h at 37 °C. Expression of EGFP in the MDA-MB-231 cells was analyzed by using the BD FACS Canto II flow cytometry equipped with the FlowJo Software (BD Biosciences, Bradford, MA, USA).

2.8. Statistical analysis

Values are represented as mean ± SD of three independent experiments. Differences between groups were analyzed using unpaired two-tailed Student's t-test.

3. Results and discussions

3.1. Design and synthesis of the LMWP–PEG–S–S–siRNA conjugate

Biomimetic design is a valid strategy that is often applied in drug delivery, in which drugs are attached to naturally derived product (presently, low molecular weight protamine) for crossing the highly regulated and restricted plasma membrane or are cloaked by materials (*e.g.* polyethylene glycol) for circumventing capture by RES, thus improving drug delivery efficiency. siRNA duplexes do not readily enter cells due to its negative charges. When it attached to LMWP which derives from a natural product, it can be delivered into cells. After the siRNA is delivered by the LMWP into the cell, the siRNA can be retained in the cytosol since our specially designed disulfide linkage between the two can be cleaved due to the elevated levels of reductase and glutathione activities in the cytosol, thereby performing gene silencing through the RISC system. Furthermore, after modified with PEG, the shielding effect on charged molecules was achieved and host immune response was reduced.

In this study, the double-chain anti-EGFP siRNA (5′-GGCUACGUCCAGGAGCGCACC-3′, 3′-UUCCGAUGCAGGUCCUCGCG U-5′) was selected as a model siRNA agent. At the same time, LMWP peptide (VSRRRRRRGGRRRR) was derived from native protamine by thermolysin digestion according to protocol in our laboratory. This compound was confirmed to possess cell-penetrating ability, and was selected as the primary representative CPP drug. As depicted in Scheme 1, hetero-bifunctional PEG derivatives NHS–PEG–MAL as a linker was introduced to conjugate the $-NH_2$ group of LMWP at the N-terminal to siRNA modified with sulfhydrylat the 5′-end in solution. It is worth noting that this approach was proposed based on the unique and unparalleled dynamic movement of PEG chain in aqueous and its shielding function. Introduction of PEG could reduce the aggregation of polycation peptides and polyanionic nucleic acids due to electrostatic interactions, while increasing the solubility of their linked compound, which has been demonstrated in our previous work[26]. In addition, prolonging blood residence, decreasing metabolic enzymes degradation and reducing protein immunogenicity were achieved *via* in their ability to reduce uptake by reticuloendothelial system through a successful PEGylation[30,31]. siRNA needs to remain in the cytosol and perform their gene silencing therapy through the RISC system. Based on this, the novel strategy of conjugation was designed coupling the 1:1 monomeric LMWP–siRNA covalent conjugate *via* a cytosol-cleavable disulfide linkage. Thiol modification by PEGylation met the goals of the project. To our knowledge, the primary coupling reactions for modification of sulfhydryls proceed by one of two routes: alkylation or disulfide interchange[32]. The double bond of maleimides may undergo an alkylation reaction with sulfhydryl groups to form stable thioether bonds. However, since a thioether bond degradation cannot occur in the cells, the gene silencing effect of siRNA delivery system would be affected. Therefore, it is necessary to undergo activation of SPDP and reduction of DTT before coupling with thiolated siRNA. To simplify the activation process, hetero-bifunctional PEG derivatives NHS–PEG–OPSS, where disulfide interchange reaction occurs, would be an excellent candidate. The PEG modified with pyridyl disulphide could be directly conjugated to siRNA containing a thiol group, since a pyridyl disulfide will readily undergo an interchange reaction with a free sulfhydryl to yield a single mixed disulfide product[33,34].

3.2. Purification of the LMWP–PEG–S–S–siRNA conjugate

Heparin cation exchange chromatography was employed to purify the LMWP–PEG–SH as well as the products of each step involved in obtaining this compound. As shown in Fig. 1A1, LMWP–PEG (MAL) conjugate and LMWP were eluted from heparin affinity column at 0.9 and 1.2 mol/L NaCl, due to skeleton of heparin column with significant negative charge and strong binding affinity towards LMWP. Because of the absence of strong binding affinity towards heparin, the excess reactants introduced in subsequent synthesis steps were directly eluted. Meanwhile, the product of each step can be eluted from the heparin column with 2 mol/L NaCl solution (Fig. 1A2 and A3).

Purification chromatographyof the crude LMWP–PEG(MAL)–siRNA conjugate is illustrated in Fig. 1B. When first purified on the heparin column, the unreacted siRNA–SH molecule and the by-product siRNA–S–S–siRNA were removed at the beginning, while LMWP–PEG(MAL)–siRNA conjugates and byproduct LMWP–PEG–S–S–PEG–LMWP were eluted with 2 mol/L NaCl solution. In the purified product solution eluted from the heparin column, the related LMWP compound and the LMWP–PEG (MAL)–siRNA conjugate were also present. For further purification, DEAE anion exchange chromatography was used to obtain pure LMWP–PEG(MAL)–siRNA conjugate. The related LMWP compound with a positive charge did not bind to the anion exchange column, while the LMWP–PEG(MAL)–siRNA conjugate would bind to the DEAE column and subsequently be eluted using a gradient NaCl solution.

Purification results using Method 2 were reported in previous studies[26]. In brief, LMWP–PEG–SH and anti-EGFP siRNA were eluted from the DEAE column at NaCl concentrations of 0 and 0.4 mol/L, while the LMWP–PEG–S–S–siRNA conjugate was eluted in-between of these two salt concentrations (0.2 mol/L).

Purification chromatographies of the LMWP–PEG(OPSS)–siRNA conjugates are shown in Fig. 2A. As seen, the LMWP–PEG(OPSS) conjugate and LMWP were eluted from heparin affinity column at 0.9 and 1.2 mol/L NaCl, presumably attributed to weaker binding affinity to the heparin column due to the PEG shielding effect. In Fig. 2B, excess LMWP–PEG(OPSS) compound was eluted at the beginning of chromatography, and the LMWP–PEG(OPSS)–siRNA conjugate was eluted from DEAE column at 0.3 mol/L NaCl due to presence of the anionic siRNA moiety on the conjugates. Moreover, the by-product siRNA–S–S–siRNA was also eluted at about 0.4 mol/L (the trailing peak in Fig. 2B), which may be attributed to the stronger polyanionic properties than siRNA alone.

3.3. The conjugation yield of related LMWP compound and LMWP–PEG–S–S–siRNA conjugate

Three methods were applied to synthesize and purify the *LMWP–PEG–S–S–siRNA* conjugate and the yields of all three methods were compared. The conjugation yields of the LMWP related compounds were obtained by quantification of the peak area (Table 1). As seen, the yields of LMWP–PEG(MAL), LMWP–PEG–Cys, LMWP–PEG–PDP, LMWP–PEG–SH, and LMWP–PEG(OPSS) were 96%, 96%, 95%, 95% and 95%, respectively. The overall yield of the purified LMWP–PEG–SH compound was 83%, whereas the yield of LMWP–PEG(OPSS) compound was

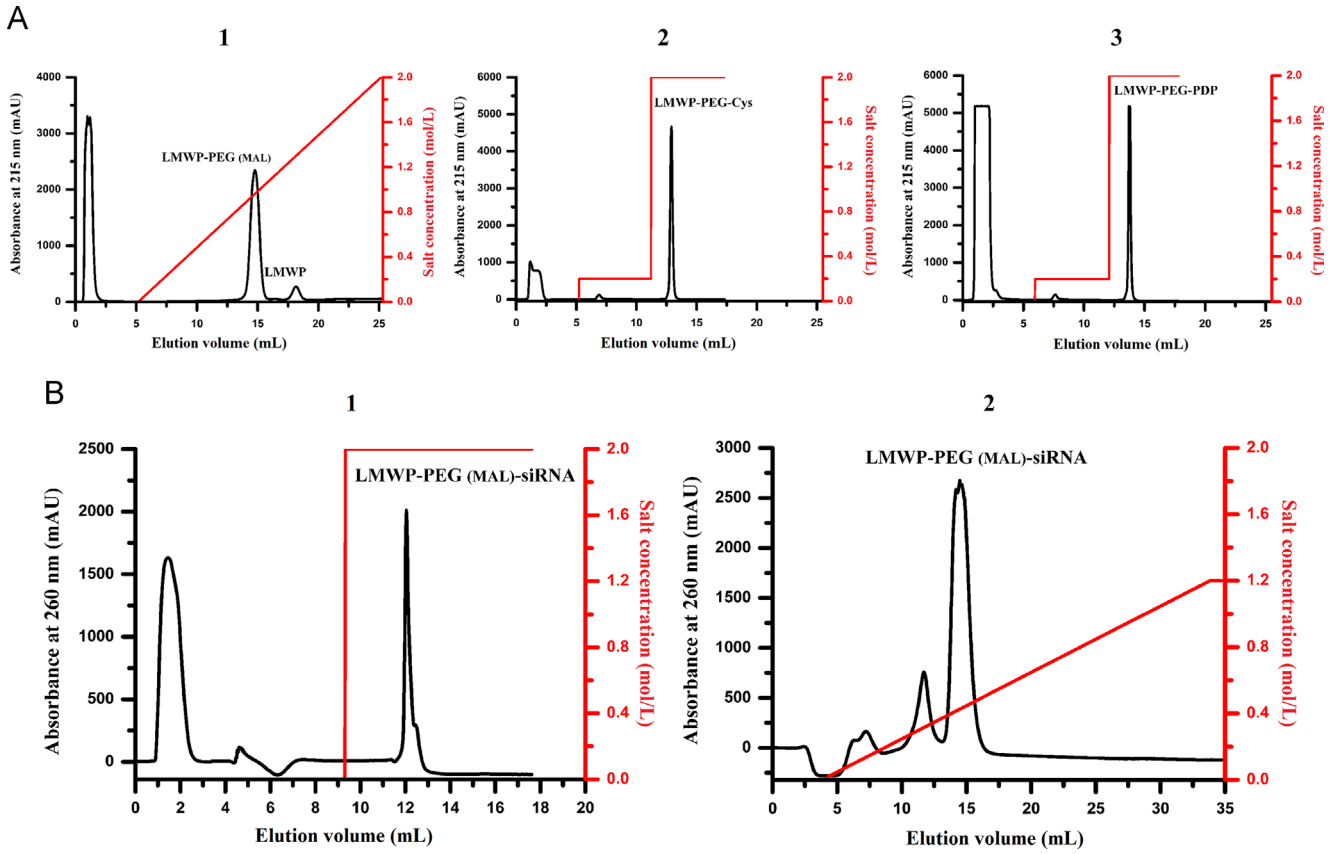

Figure 1 Purification chromatography of the LMWP–PEG(MAL)–siRNA conjugate. (A) Purification of the LMWP–PEG–SH compound through heparin chromatograms: (1) LMWP–PEG(MAL); (2) LMWP–PEG–Cys; (3) LMWP–PEG–PDP. (B) Purification of LMWP–PEG(MAL)–siRNA conjugate by ion exchange chromatography: (1) heparin affinity column; (2) DEAE column.

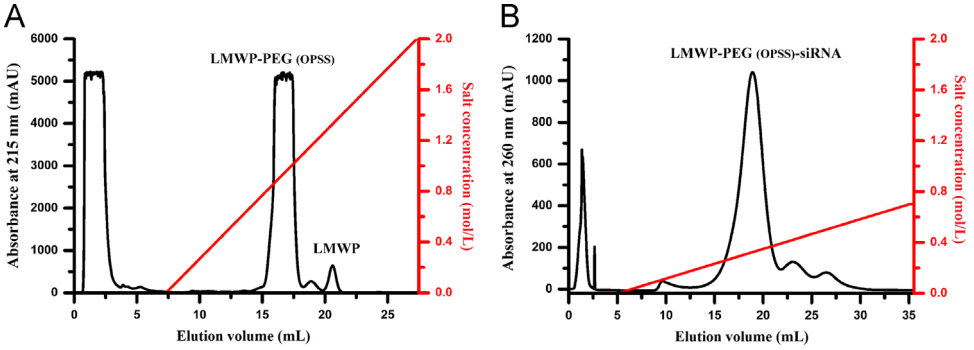

Figure 2 Purification the LMWP–PEG(OPSS)–siRNA conjugate through ion exchange chromatography: (A) heparin chromatograms of LMWP–PEG(OPSS); (B) DEAE chromatograms of LMWP–PEG(OPSS)–siRNA conjugate.

Table 1 Yields of the LMWP-related compounds.

Reaction intermediate	Ingredients of each step	Yield (%)[a]	Total Yield (%)
LMWP–PEG–SH compound	LMWP–PEG(MAL)	96	83
	LMWP–PEG–Cys	96	
	LMWP–PEG–PDP	95	
	LMWP–PEG–SH	95	
LMWP–PEG(OPSS) compound	LMWP–PEG(OPSS)	95	95

[a]The yields of the LMWP compounds were spectrophotometrically calculated on the basis of absorbance at 215 nm wavelength.

Table 2 Yields of LMWP–PEG–S–S–siRNA conjugates.

Method	Functional linker	Purification step (columns)	Yield (%)[a]
1	NHS–PEG–MAL (~3500 Da)	Heparin affinity column DEAE column	13
2	NHS–PEG–MAL (~3500 Da)	DEAE column	30
3	NHS–PEG–OPSS (~3500 Da)	DEAE column	48

[a]The yields of the siRNA were determined by measuring the absorbance at 260 nm after purification.

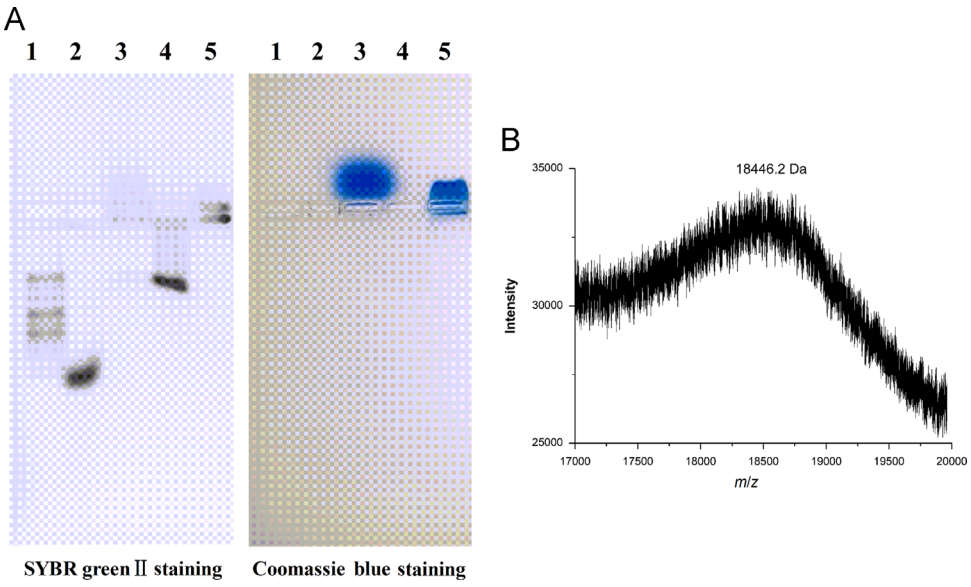

Figure 3 Characterization of the LMWP–PEG(OPSS)–siRNA conjugate. (A) An agarose gel (2%) electrophoretic identify of conjugate. The samples containing: (1) 20 bp marker, (2) anti-EGFP siRNA alone, (3) LMWP–PEG, (4) the LMWP–PEG–S–S–anti-EGFP siRNA conjugate, and (5) physical mixture (molar ratio: 1:1) of LMWP and anti-EGFP siRNA. (B) MALDI-TOF results for the LMWP–PEG(OPSS)–siRNA conjugate.

95% as seen in Table 1. It revealed that the level of yield was affected by the number of synthesis steps, although the yield of each step for the first method was as high as 95%.

The yields of the LMWP–PEG–S–S–siRNA conjugate targeted to the *EGFP* gene were shown in Table 2. The overall yields of the siRNA produced by different methods were 13%, 30%, 48% respectively. Compared with Method 1 (Scheme 1A1), Method 2 (Scheme 1A2) improves the yield of siRNA because of its reduced purification step. Yet, compared with Method 3, it should be noted that for the final conjugation reactions, LMWP-SH compound employed in Method 2 produced more by-products such as LMWP–PEG–S–S–PEG–LMWP, which affected the final yield of the conjugates. Our findings indicate that the LMWP–PEG–S–S–siRNA conjugate synthesized by the LMWP–PEG(OPSS) compound showed the highest yield up to 48% by simplifying the synthesis and purification step, which provides a basis for future large-scale production.

3.4. *Characterization of LMWP–PEG–S–S–siRNA conjugates*

Results of the agarose gel electrophoresis analysis of the conjugates after purification by ion exchange chromatography confirmed the successful synthesis of the desired LMWP–PEG (OPSS)–siRNA conjugate (Fig. 3A). For better observation, the agarose gel was stained with SYBR green II to show the bands of products containing nucleic acid, and then stained with Coomassie Brilliant Blue to show the bands of products containing protein. On one hand, our results showed that after conjugation with LMWP-PEG, the migration rate of LMWP–PEG(OPSS)–siRNA conjugates (Lane 4) were significantly slower than that of free siRNA (Lane 2). On the other hand, compared with LMWP–PEG (Lane 3) and LMWP/siRNA complexes (Lane 5), the migration rate of siRNA conjugates (Lane 4) was significantly faster. All these results suggested that successful conjugation of LMWP–PEG and siRNA occurred. Furthermore, the band of conjugate (Lane 4) showed at higher MW than that of monomeric conjugate, which can be attributed to the presence of PEG in the conjugate, in agreement with results report by other investigator[5].

MALDI-TOF data for the LMWP–PEG–S–S–siRNA product is presented in Fig. 3B. Analysis yielded a molecular weight of 18446.2 Da, in agreement with the calculated molecular weight for this product, confirming the successful synthesis of the monomeric LMWP–PEG–S–S–siRNA conjugate.

3.5. *The size and ζ-potential of LMWP–PEG–S–S–siRNA conjugates*

As displayed in Fig. 4A, the average particle size of the LMWP–PEG–S–S–siRNA conjugate was 2.491 ± 0.17 nm, suggesting that the final conjugate existed in a hydrated and soluble state.

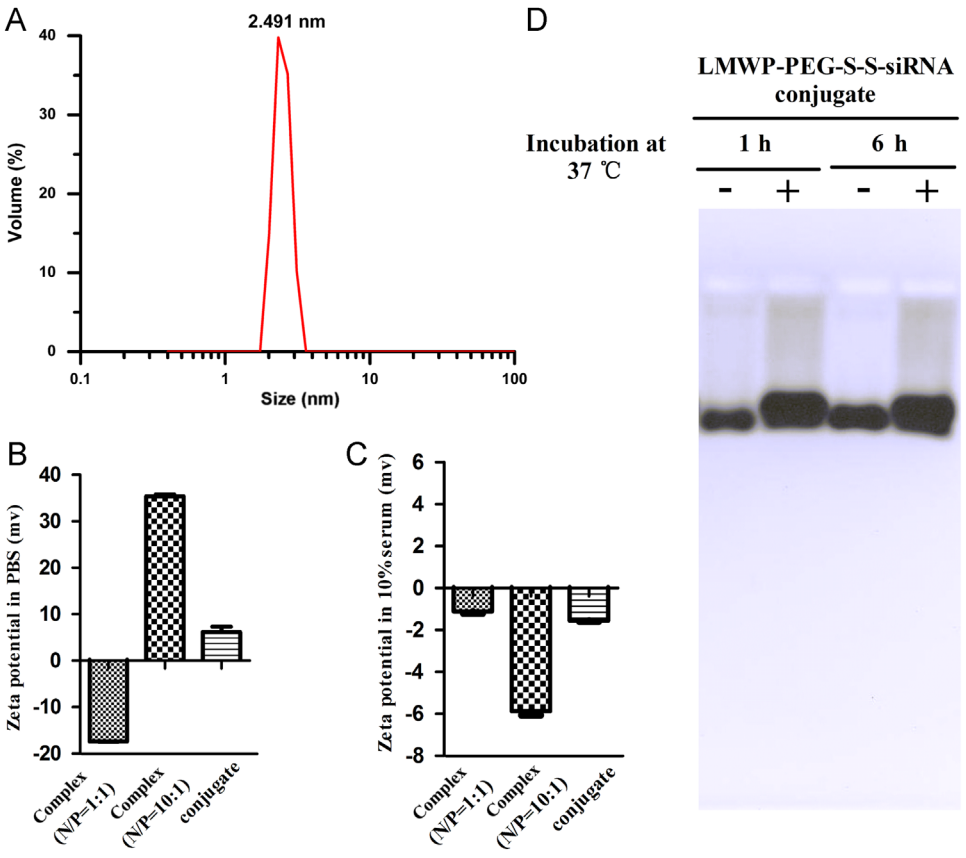

Figure 4 Properties of LMWP–PEG–S–S–siRNA conjugate. (A) Particle size of the conjugate. ζ-Potential of the conjugate, complex (*N/P* = 1:1) and complex (*N/P* = 10:1) in (B) PBS and (C) 10% serum. (D) Gel retardation assays for determination stability of conjugate in serum after 1 and 6 h at 37 °C. Here, + represents the conjugate exposed to the serum, and – represents the conjugate exposed to the phosphate buffer.

We assessed the charge of the LMWP–PEG–S–S–siRNA conjugate in different media. In phosphate buffer , we observed large differences between the complexes that correlate with the charge ratio of 1 and 10. At high charge ratios, a pronounced positive ζ-potential was found for the complexes. The ζ-potentials of the LMWP–PEG–S–S–siRNA conjugate were also positive (Fig. 4B). The positive surface charges are commonly believed to allow interaction with the polyanionic glycosaminoglycans on cell surface[35].

However, the charges of all of the products were negative in the presence of serum (Fig. 4C). The change in ζ-potential was probably caused by the serum proteins interaction with the outer layer of the conjugate and complex. This result is consistent with the reported observations[36]. It was believed that the uptake of these products was mediated by scavenger receptors, a type of cell surface receptor involved in the cellular uptake of negatively charged macromolecules.

3.6. The stability of LMWP–PEG–S–S–siRNA conjugates in the presence of serum

During circulation in the bloodstream, the LMWP–PEG–S–S–siRNA conjugate will interact with serum proteins. In the bloodstream, premature disintegration would be detrimental, leading to degradation of the siRNA. In fact, rapid degradation by nucleases is one of the major limitations of current siRNA delivery strategies.

In this paper, serum stability of the LMWP–PEG–S–S–siRNA conjugate was assessed over a 6 h time course. The conjugate was detectable as a high-molecular-weight band showing only minor intensity changes after serum exposure (Fig. 4D).

3.7. Intracellular uptake of LMWP–PEG–S–S–siRNA conjugates

The cell penetrating properties of LMWP–PEG(OPSS)–siRNA was examined by uptake studies in HCT116 cells utilizing TAMRA-labeled siRNA samples. Three samples including: (1) PBS, (2) anti-EGFP siRNA alone, and (3) LMWP–PEG(OPSS)–siRNA conjugate. The confocal images of HCT 116 cells taken after incubation with these samples are shown in Fig. 5A. As a control, the TAMRA–siRNA alone was employed for uptake studies, and only weak fluorescence signal was captured as expected. Compared with the background fluorescence intensity (FI = 870) shown by the PBS buffer, the TAMRA-labeled anti-EGFP siRNA displayed slightly higher yet still fairly weak cellular TAMRA intensities (FI = 5893.8; Fig. 5B). The lack of cell uptake of TAMRA–siRNA alone is consistent with our previous findings and confirmed by other literature[37–39]. This is primarily because siRNAs are anionic macromolecules that do not readily enter cells. Strong fluorescence intensity (FI = 210269.5) was clearly observed inside the cells that were treated with LMWP–PEG(OPSS)–siRNA conjugate. Overall, cellular uptake of the LMWP–PEG–S–S–siRNA conjugate was 35.6-fold higher than that displayed by native siRNA without LMWP modification. Furthermore, the merged image of the conjugate suggested that the location of conjugate was mainly in the cytosol. It revealed that the disulfide bond of the conjugate induced by the disulfide interchange reaction was also effectively broken down under the cytoplasmic reducing environment, in agreement with the results obtained with the conjugates synthesized

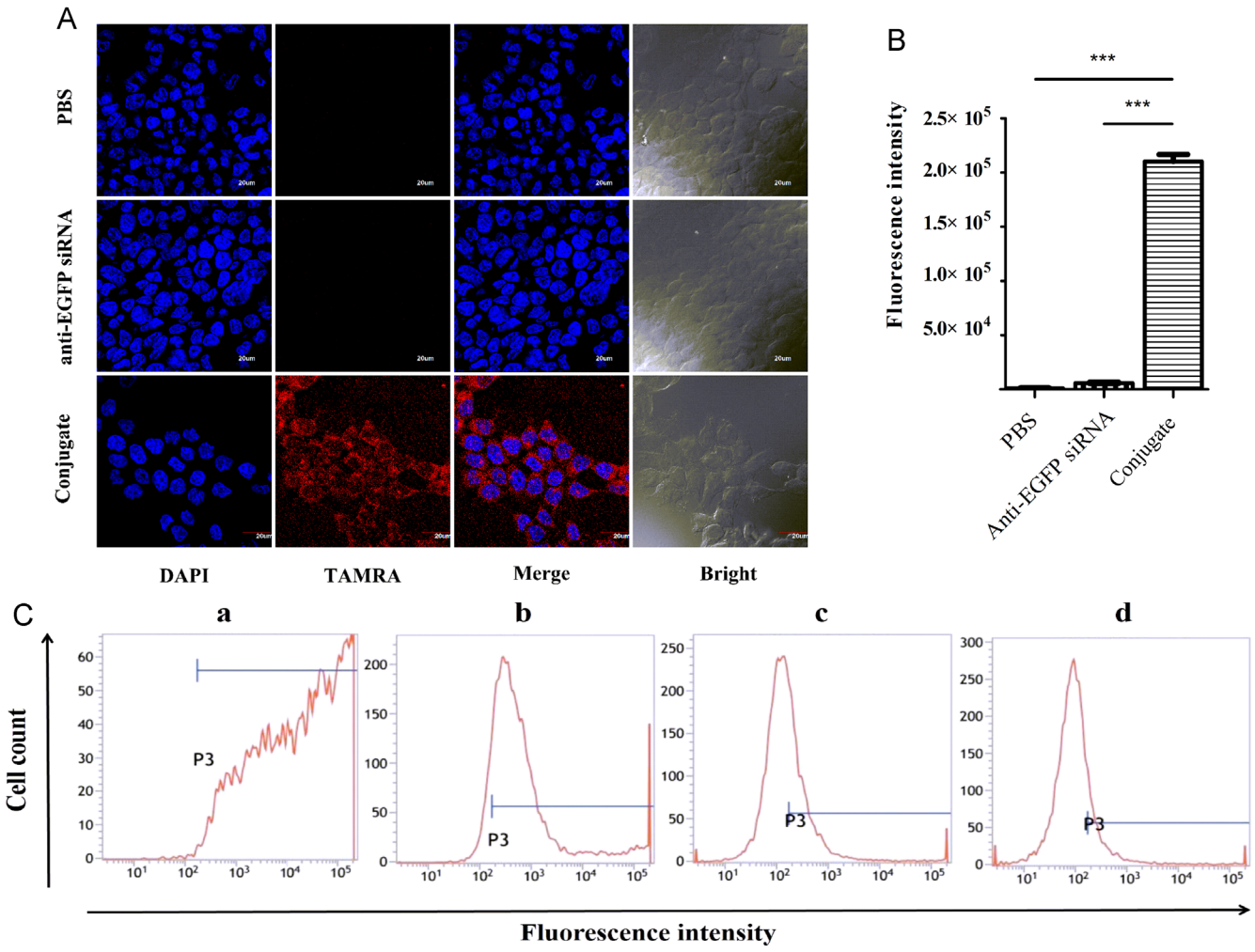

Figure 5 Cellular uptake studies carried out on HCT 116 cells using TAMRA-labeled anti-EGFP siRNA, and the gene silencing down effect by anti-EGFP siRNA on EGFP over-expressed steady transfection MDA-MB-231-EGFP cells. The cells were all treated with PBS; anti-EGFP siRNA alone; LMWP–PEG–S–S–siRNA conjugate. (A) Representative confocal microscopy images of the HCT 116 cells. Scale bars, 20 μm. (B) Fluorescence intensity of confocal image results, the values shown represent the mean ± SD ($n = 3$, $^{***}P < 0.001$). (C) FACS quantification analysis gene silencing results. The test samples are: (a) PBS, (b) anti-EGFP siRNA alone, (c) LMWP/siRNA complex, and (d) the LMWP–PEG–S–S–anti-EGFP siRNA conjugate.

from LMWP–PEG–SH by Methods 1 and 2. From this point of view, the conjugates synthesized from the simplified Method 3 was as effective as the original conjugates in terms of cell uptake efficiency and cytoplasmic release, which plays an important role in the delivery of siRNAs.

3.8. In vitro gene silencing efficacy of LMWP–PEG–S–S–siRNA conjugates

The gene silencing efficacy of LMWP–PEG–S–S–siRNA conjugate was examined by flow cytometry in MDA-MB-231-EGFP cells. The results presented in Fig. 5C revealed that the levels of EGFP expression in the MDA-MB-231-EGFP cells treated with naked anti-EGFP siRNA (sample b) and LMWP/siRNA complex (sample c) were 91.64% and 41.32%, respectively, of the background FACS number shown by cells treated with PBS (sample a). As expected, the LMWP–PEG–S–S–siRNA conjugate yielded the most obvious down-regulation on EGFP expression to 21.21%.

CPPs can convey their cargo into cells by two principally different mechanisms—endocytosis and direct translocation[40]. Additionally, CPPs may utilize different pathways depending on the respective conditions, such as the type of CPP, type of cargo molecules and type of target cell. An example of arginine-rich peptide Tat has been demonstrated that its internalization is independent of endocytosis and occurs without disruption of the cell membrane[41]. In other studies, the internalized TATU1A/U1A–siRNA complexes seemed completely trapped in the endosomes, and did not induce gene silencing, while the TAT–siRNA conjugate induced much better gene silencing effect[40,42]. In our study, the conjugate also yielded more effective gene silencing effect than the physical complexes, which may be attributed to low endosomal uptake or better endosomal escape. Further studies will be conducted to clarify this mechanism.

4. Conclusions

It is worth noting that the real bottleneck to achieve successful intracellular siRNA delivery *in vivo* lies in the inability to

synthesize sufficient quantity of the CPP–siRNA covalent conjugates. Presently, we demonstrate feasible methods to overcome this limitation. We developed a general and robust approach to synthesize the LMWP–siRNA covalent conjugate, in which the hetero-bifunctional PEG derivate NHS–PEG–OPSS was introduced innovatively, simplifying the synthetic process. We performed comparative studies of synthesis and purification methods and compared the yields of conjugates. These findings confirmed that the proposed novel conjugation strategies would not only provide diverse approaches for conjugation, but also produce higher yields. Thus far, none of the reported methods are available to produce covalent 1:1 CPP:siRNA chemical conjugate without encountering the charge-induced aggregation/precipitation between the cationic CPP and anionic siRNA, not to mention producing sufficient quantities of the final CPP–siRNA conjugates that were linked with a cytosol-cleavable disulfide linkage. These features by themselves are great innovation for carrying out *in vivo* and subsequent clinical trials. Therefore, the proposed conjugation strategy paves the road for future clinical translation of the siRNA therapeutic agents. In addition, NHS–PEG–OPSS was introduced to increase the efficiency of the coupling reaction and the strategy of purification was improved to reduce the formation of the byproduct siRNA–S–S–siRNA that also improved the final yield. These improvements make this method suitable for mass production to meet the needs of chemicals in animal studies and clinical efficacy trials. Furthermore, we demonstrated *in vitro* that the LMWP–PEG–S–S–siRNA conjugate prepared by our simplified synthesis strategy exhibited successful cellular uptake of the siRNA agents and potent gene silencing effects.

However, effective *in vivo* delivery of these conjugates requires a carefully designed delivery system that can protect the conjugates from proteolytic degradation thereby maintaining their stability *in vivo*, as well as enhancing the tumor targeting efficiency and reducing the systemic toxic effects to normal tissues. To this regard, integration of these covalent conjugates with our ongoing research of designing a magnetic iron oxide nano-carrier (MION)-based delivery system is essential to achieve the milestone goal of realizing a MRI-guided, cocktail-type siRNA brain tumor therapy. Since each conjugate contains only a single PEG molecule, similar to that of many clinically approved PEG–drug conjugates [*e.g.* pegylated asparaginase in acute lymphoblastic leukemia (ALL)], this low amount of PEG is not going to cause toxicity concerns; as being approved for clinical use for many PEGylated drug conjugates. Overall, the current study has convinced us that the proposed coupling strategy can serve as a tool for siRNA delivery and can overcome the problem of deficient quantity of the CPP–siRNA covalent conjugates *in vitro*. The present work therefore paves the promising avenue towards siRNA biomimetic delivery and future clinical translation.

Acknowledgements

This research was sponsored in part by National Key Research and Development Plan (2016YFE0119200). This work was also partially supported by the National Natural Science Foundation of China (NSFC) on Grants 81402856 and 81361140344 (A3 project), Tianjin Municipal Science and Technology Commission (Grant 15JCYBJC28700) and the National Key Basic Research Program of China (Grant 2013CB932502).

References

1. Fire A, Xu S, Montgomery MK, Kostas SA, Driver SE, Mello CC. Potent and specific genetic interference by double-stranded RNA in *Caenorhabditis elegans*. *Nature* 1998;**391**:806–11.
2. Kumar P, Ban HS, Kim SS, Wu H, Pearson T, Greiner DL, et al. T cell-specific siRNA delivery suppresses HIV-1 infection in humanized mice. *Cell* 2008;**134**:577–86.
3. Pardridge WM. shRNA and siRNA delivery to the brain. *Adv Drug Deliv Rev* 2007;**59**:141–52.
4. Zhao J, Mi Y, Feng SS. Targeted co-delivery of docetaxel and siPlk1 by herceptin-conjugated vitamin E TPGS based immunomicelles. *Biomaterials* 2013;**34**:3411–21.
5. Zhu L, Mahato RI. Targeted delivery of siRNA to hepatocytes and hepatic stellate cells by bioconjugation. *Bioconjug Chem* 2010;**21**:2119–27.
6. Wang J, Lu Z, Wientjes MG, Au JL. Delivery of siRNA therapeutics: barriers and carriers. *AAPS J* 2010;**12**:492–503.
7. Gavrilov K, Saltzman WM. Therapeutic siRNA: principles, challenges, and strategies. *Yale J Biol Med* 2012;**85**:187–200.
8. Guo P, Yang J, Jia D, Moses MA, Auguste DT. ICAM-1-targeted, Lcn2 siRNA-Encapsulating liposomes are potent anti-angiogenic agents for triple negative breast cancer. *Theranostics* 2016;**6**:1–13.
9. Fan B, Kang L, Chen L, Sun P, Jin M, Wang Q, et al. Systemic siRNA delivery with a dual pH-responsive and tumor-targeted nanovector for inhibiting tumor growth and spontaneous metastasis in orthotopic murine model of breast carcinoma. *Theranostics* 2017;**7**:357–76.
10. Van Asbeck AH, Beyerle A, McNeill H, Bovee-Geurts PH, Lindberg S, Verdurmen WP, et al. Molecular parameters of siRNA–cell penetrating peptide nanocomplexes for efficient cellular delivery. *ACS Nano* 2013;**7**:3797–807.
11. Kubo T, Yanagihara K, Takei Y, Mihara K, Sato Y, Seyama T. Lipid-conjugated 27-nucleotide double-stranded RNAs with dicer-substrate potency enhance RNAi-mediated gene silencing. *Mol Pharm* 2012;**9**:1374–83.
12. Eguchi A, Dowdy SF. siRNA delivery using peptide transduction domains. *Trends Pharmacol Sci* 2009;**30**:341–5.
13. Yoo JW, Irvine DJ, Discher DE, Mitragotri S. Bio-inspired, bioengineered and biomimetic drug delivery carriers. *Nat Rev Drug Discov* 2011;**10**:521–35.
14. Ozpolat B, Sood AK, Lopez-Berestein G. Liposomal siRNA nanocarriers for cancer therapy. *Adv Drug Deliv Rev* 2014;**66**:110–6.
15. Gilleron J, Querbes W, Zeigerer A, Borodovsky A, Marsico G, Schubert U, et al. Image-based analysis of lipid nanoparticle-mediated siRNA delivery, intracellular trafficking and endosomal escape. *Nat Biotechnol* 2013;**31**:638–46.
16. Ding Y, Wang W, Feng M, Wang Y, Zhou J, Ding X, et al. A biomimetic nanovector-mediated targeted cholesterol-conjugated siRNA delivery for tumor gene therapy. *Biomaterials* 2012;**33**:8893–905.
17. Kozielski KL, Tzeng SY, De Mendoza BA, Green JJ. Bioreducible cationic polymer-based nanoparticles for efficient and environmentally triggered cytoplasmic siRNA delivery to primary human brain cancer cells. *ACS Nano* 2014;**8**:3232–41.
18. Herrmann A, Priceman SJ, Kujawski M, Xin H, Cherryholmes GA, Zhang W, et al. CTLA4 aptamer delivers STAT3 siRNA to tumor-associated and malignant T cells. *J Clin Invest* 2014;**124**:2977–87.
19. Alam MR, Ming X, Fisher M, Lackey JG, Rajeev KG, Manoharan M, et al. Multivalent cyclic RGD conjugates for targeted delivery of small interfering RNA. *Bioconjug Chem* 2011;**22**:1673–81.
20. Choi YS, Lee JY, Suh JS, Kwon YM, Lee SJ, Chung JK, et al. The systemic delivery of siRNAs by a cell penetrating peptide, low molecular weight protamine. *Biomaterials* 2010;**31**:1429–43.
21. Lehto T, Kurrikoff K, Langel Ü. Cell-penetrating peptides for the delivery of nucleic acids. *Expert Opin Drug Deliv* 2012;**9**:823–36.

22. Lee SH, Kang YY, Jang HE, Mok H. Current preclinical small interfering RNA (siRNA)-based conjugate systems for RNA therapeutics. *Adv Drug Deliv Rev* 2016;**104**:78–92.
23. Wadia JS, Stan RV, Dowdy SF. Transducible TAT–HA fusogenic peptide enhances escape of TAT-fusion proteins after lipid raft macropinocytosis. *Nat Med* 2004;**10**:310–5.
24. Reischl D, Zimmer A. Drug delivery of siRNA therapeutics: potentials and limits of nanosystems. *Nanomedicine* 2009;**5**:8–20.
25. Sawant R, Torchilin V. Intracellular transduction using cell-penetrating peptides. *Mol Biosyst* 2010;**6**:628–40.
26. Ye J, Liu E, Gong J, Wang J, Huang Y, He H, et al. High-Yield synthesis of monomeric LMWP(CPP)–siRNA covalent conjugate for effective cytosolic delivery of siRNA. *Theranostics* 2017;**7**:2495–508.
27. David AE, Gong J, Chertok B, Domszy RC, Moon C, Park YS, et al. Immobilized thermolysin for highly efficient production of low-molecular-weight protamine-an attractive cell-penetrating peptide for macromolecular drug delivery applications. *J Biomed Mater Res A* 2012;**100**:211–9.
28. He H, Ye J, Liu E, Liang Q, Liu Q, Yang VC. Low molecular weight protamine (LMWP): a nontoxic protamine substitute and an effective cell-penetrating peptide. *J Control Release* 2014;**193**:63–73.
29. Shimizu H, Jinno F, Morohashi A, Yamazaki Y, Yamada M, Kondo T, et al. Application of high-resolution ESI and MALDI mass spectrometry to metabolite profiling of small interfering RNA duplex. *J Mass Spectrom* 2012;**47**:1015–22.
30. Kolate A, Baradia D, Patil S, Vhora I, Kore G, Misra A. PEG-a versatile conjugating ligand for drugs and drug delivery systems. *J Control Release* 2014;**192**:67–81.
31. Torchilin VP. Multifunctional, stimuli-sensitive nanoparticulate systems for drug delivery. *Nat Rev Drug Discov* 2014;**13**:813–27.
32. Veronese FM, Pasut G. PEGylation, successful approach to drug delivery. *Drug Discov Today* 2005;**10**:1451–8.
33. Heredia KL, Nguyen TH, Chang CW, Bulmus V, Davis TP, Maynard HD. Reversible siRNA–polymer conjugates by RAFT polymerization. *Chem Commun* 2008;**2008**:3245–7.
34. Ma D, Tian S, Baryza J, Luft JC, De Simone JM. Reductively responsive hydrogel nanoparticles with uniform size, shape, and tunable composition for systemic siRNA delivery *in vivo*. *Mol Pharm* 2015;**12**:3518–26.
35. Ziegler A, Seelig J. Binding and clustering of glycosaminoglycans: a common property of mono- and multivalent cell-penetrating compounds. *Biophys J* 2008;**94**:2142–9.
36. Ezzat K, Helmfors H, Tudoran O, Juks C, Lindberg S, Padari K, et al. Scavenger receptor-mediated uptake of cell-penetratingpeptide nanocomplexes with oligonucleotides. *FASEB J* 2012;**26**:1172–80.
37. Du J, Sun Y, Shi QS, Liu PF, Zhu MJ, Wang CH, et al. Biodegradable nanoparticles of mPEG–PLGA–PLL triblock copolymers as novel non-viral vectors for improving siRNA delivery and gene silencing. *Int J Mol Sci* 2012;**13**:516–33.
38. Malmo J, Sandvig A, Vårum KM, Strand SP, et al. Nanoparticle mediated p-glycoprotein silencing for improved drug delivery across the blood–brain barrier: a siRNA–chitosan approach. *PLoS One* 2013;**8**:e54182.
39. Liu X, Liu C, Zhou J, Chen C, Qu F, Rossi JJ, et al. Promoting siRNA delivery *via* enhanced cellular uptake using an arginine-decorated amphiphilic dendrimer. *Nanoscale* 2015;**7**:3867–75.
40. Endoh T, Ohtsuki T. Cellular siRNA delivery using cell-penetrating peptides modified for endosomal escape. *Adv Drug Deliv Rev* 2009;**61**:704–9.
41. Ter-Avetisyan G, Tünnemann G, Nowak D, Nitschke M, Herrmann A, Drab M, et al. Cell entry of arginine-rich peptides is independent of endocytosis. *J Biol Chem* 2009;**284**:3370–8.
42. Erazo-Oliveras A, Muthukrishnan N, Baker R, Wang TY, Pellois JP. Improving the endosomal escape of cell-penetrating peptides and their cargos: strategies and challenges. *Pharmaceuticals* 2012;**5**:1177–209.